



A novel observer design for friction estimation

Caner Odabaş & Ömer Morgül

To cite this article: Caner Odabaş & Ömer Morgül (2024) A novel observer design for friction estimation, International Journal of Control, 97:6, 1418-1431, DOI: [10.1080/00207179.2023.2207690](https://doi.org/10.1080/00207179.2023.2207690)

To link to this article: <https://doi.org/10.1080/00207179.2023.2207690>



Published online: 10 May 2023.



Submit your article to this journal [↗](#)



Article views: 208



View related articles [↗](#)





View Crossmark data [↗](#)



Citing articles: 1 View citing articles [↗](#)



A novel observer design for friction estimation

Caner Odabaş ^{a,b} and Ömer Morgül ^a

^aDepartment of Electrical and Electronics Engineering, Bilkent University, Ankara, Turkey; ^bASELSAN Radar, Electronic Warfare and Intelligence Systems Department, Ankara, Turkey

ABSTRACT

In this paper, we propose a novel adaptive friction estimator for simple mechanical systems with Coulomb friction. We assume that the friction constant is unknown and we propose an adaptive observer for its estimation. We show that under certain conditions the observer structure is asymptotically stable. The proposed observer dynamics has two tuning parameters and essentially behaves as a second-order switching system. These parameters could be utilised to tune some time domain performance measures such as settling time, per cent overshoot, etc., under certain conditions. Lastly, simulations reveal that when the actual friction is not confined to Coulomb friction only, the proposed design improves the position tracking performance, especially when the position controller has low bandwidth.

ARTICLE HISTORY

Received 25 January 2022
Accepted 12 April 2023

KEYWORDS

Friction observer; adaptive control; switching systems; dwell-time

1. Introduction

Friction is an unavoidable opposing force/torque that can directly affect mechanical systems' performance or even stability. Therefore, friction cancellation can be a vital issue for precise position control. Friction exists due to complex interaction between two surfaces in contact and exhibits different characteristics in every motion phase. Therefore, there are different approaches to model friction behaviour. Among these models, Coulomb friction is a well-known simple static model that describes the fundamental and dominant component of friction at the steady-state. This static model can be improved by including the Stribeck Effect and viscous friction to obtain a more realistic and continuous model (Olsson et al., 1998). Nonetheless, static friction models generally well portray the sliding phase, which can be treated as steady-state characteristics of friction. However, they are mostly inadequate to express pre-sliding friction characteristics such as break-away force, stick-slip motion, friction lag. In this sense, dynamic models can express the pre-sliding phase of motion to a better extent compared to static models thanks to time-varying model parameters. Therefore, for simulations of aerospace applications, Dahl developed a dynamic model for sliding and rolling friction in 1968 (Dahl, 1968). This model has an advantage in capturing hysteresis and pre-sliding displacement behaviours since it formulates friction as a function of the displacement and the sign of velocity. However, it does not include the Stribeck effect and viscous friction. Bliman and Sorine have developed another model based on linear space invariant differential operators to overcome these drawbacks (Bliman & Sorine, 1993). Unfortunately, this model exhibits a spatially transient Stribeck effect when the direction of motion is changed but not in the steady state. Thus, another extension is introduced by the scientists from the universities of Lund and Grenoble. Therefore, this model is named the LuGre friction model (Canudas de Wit et al., 1995).

In the literature, the LuGre model is a prevalent dynamic model capturing pre-sliding characteristics in addition to steady-state components of the friction such as the Stribeck Effect and viscous friction. Indeed, one can find much more examples of friction models at different complexities in the literature, see Armstrong-Hélouvry et al. (1994) and the references therein for more examples. Certainly, accurate parameter identification may be challenging for the advanced friction models, especially if the model compromises many coefficients.

Mainly, there are two different approaches to friction cancellation, namely, model-based and non-model-based approaches. Dithering and joint control are some examples of non-model based friction compensation methods. On the other hand, much more examples of model-based approaches exist in the literature (Armstrong-Hélouvry et al., 1994). Generally, as the name implies, precise identification of friction parameters is vital for model-based friction cancellation techniques. For instance, in fixed friction compensation, one considers an appropriate friction model with accurately identified coefficients to superpose via either feedback or feedforward to control input delivered to the plant. In that case, the effects of the friction existing in the positioning system can be eliminated and generated control input is completely directed to the plant as if there is no friction. Note that the steady-state characteristics of friction are related to velocity; therefore, one can conduct constant velocity tests to obtain a friction-velocity map and determine viscous coefficient, Stribeck velocity, Coulomb and stiction coefficients (Odabaş, 2021). On the other hand, dynamic characteristics of the friction in the pre-sliding stage are a function of position. Identifying these parameters is challenging and requires some advanced techniques. As an example, one can design a two-layer neural network in order to obtain precise and offline estimation using the Extended Kalman Filter (EKF) (Hensen, 2002). A similar grey box identification approach is to define a polytopic

model consisting of several locally valid friction models in order to enhance the identification performance (Hensen, 2002). Alternatively, frequency domain identification is achieved by exciting the system with random noise (Hensen, 2002). Moreover, biologically inspired Genetic and Novel Evolutionary Algorithm (NEA) can be employed to improve the accuracy of dynamical parameter identification (Tan et al., 2007; Wang & Wang, 2011). Nevertheless, such approaches might be exhaustive since the data collection process generally requires much time and a detailed setup. What is more, friction parameters tend to vary due to environmental properties such as temperature, lubricity and load (Åström & Wittenmark, 2013). Therefore, observer-based adaptive schemes are prevalent in the literature.

Particularly, LuGre Model includes an immeasurable internal state variable, z_d , in addition to its dynamic damping and stiffness coefficients. To this end, a sliding-mode observer is designed to estimate the internal state in LuGre model by Xie (2007). Hence, considering estimated z_d , an adaptive controller drives the position and velocity of the servo motor for reference tracking. In another approach, Lee and Tomizuka utilise a feedforward static friction compensation together with a Q-filter based disturbance observer to compensate for the mismatch between the actual output and the output of the nominal model in order to eliminate unmodelled friction dynamics and other disturbance signals (Lee & Tomizuka, 1996). Similarly, Olsson and Åström design a LuGre model-based friction observer, which adaptively tunes its initial parameters to minimise the modeling errors (Olsson & Astrom, 1996). Indeed, all these techniques require a friction model and identification process to some extent. Also, some observer designs do not require a priori friction estimation for estimation. For instance, as a non-model-based method, Extended Kalman-Bucy Filter (EKF) is utilised (Ray et al., 2001). A passivity-based multi-input multi-output (MIMO) controller is utilised with an observer operating as an integrator to obtain zero steady-state error for a robotic platform (Le Tien et al., 2008). Although Friedland-Park observer fundamentally aims at Coulomb coefficient estimation, simulations and experiments reveal that it may still perform satisfactorily even if actual friction is not confined to Coulomb friction only (Friedland & Park, 1992; Odabaş & Morgül, 2014). Furthermore, the original Friedland-Park Friction Observer can be characterised by a general class of nonlinear functions that could be used as an adaptive rule in friction estimation (Odabaş, 2014). In many cases, friction compensation schemes count on velocity measurements with a good resolution and negligible time delay. Thus, rational function approximations and numerical differential equation solver based and velocity predictor schemes might be utilised in systems with considerable measurement delay (Odabaş & Morgül, 2020). Likewise, separate velocity predictor designs are provided when the direct velocity measurement of the system is not available (Palli & Melchiorri, 2008; Tafazoli et al., 1998).

In this study, our main contribution is to design a novel adaptive observer scheme to estimate the Coulomb coefficient without prior parameter identification. Simulation results show that the proposed observer can provide a promising performance under other friction models in addition to the simple Coulomb

Model. Distinctively, we assume that velocity is measurable yet still integrate the velocity predictor in the proposed adaptive friction observer to enhance the estimation performance, especially under velocity uncertainties. Compared to approaches mentioned earlier, in certain cases, one can readily determine observer parameters by considering the friction estimation's overshoot and settling time properties without any complex parameter identification or design process. This new observer describes a second-order switching system behaviour; therefore, we use some general results to show asymptotic stability under certain regularity and assumptions regarding the switching signal.

This paper is organised as follows. In the next section, we introduce observer dynamics and discuss the choice of the observer parameters. Then, we provide a stability analysis and provide sufficient conditions which guarantee asymptotic stability. Section 3 considers the integral of the time-weighted absolute error (ITAE) index to design position controller. In Section 4, we perform extensive simulations to show the effectiveness of the introduced observer under LuGre and Coulomb friction models. We also investigate the relation between controller bandwidth and the proposed friction cancellation structure and present concluding remarks.

2. Proposed adaptive observer design

In this study, we design a novel adaptive friction observer aiming at Coulomb parameter estimation. The proposed observer simultaneously takes friction and velocity dynamics into account to improve the friction estimation performance.

2.1 Dynamics

Equation of motion for a simple mechanical system under friction can be obtained as

$$J\dot{w} = -F(w) + u. \quad (1)$$

where J , w , $F(w)$ and u represent the moment of inertia, angular velocity of the system, acting friction torque and control input, respectively. Certainly, it is also possible to apply our approach for linear motion cases without losing generality. For simplicity, we assume that existing friction torque is confined to Coulomb Model such that $F(w) = J a_c \text{sgn}(w)$ where a_c stands for Coulomb coefficient and $\text{sgn}(\cdot)$ is signum function. Then, we consider designing an observer for velocity estimation first, even when w is measurable. Certainly, one may argue that such an estimation is not necessary; however, it will become apparent in the sequel that it is instrumental in estimating the friction coefficient a_c . To this end, for the system given by (1), we first propose the following velocity observer:

$$J\dot{\hat{w}} = -J\hat{a}_c \text{sgn}(w) + KJ(w - \hat{w}) + u. \quad (2)$$

where \hat{w} is the estimated angular velocity, \hat{a}_c is the estimated Coulomb friction constant and $K > 0$ is an observer gain. Note that in this framework, we define the friction estimation \hat{F}

as follows:

$$\hat{F}(w) = J\hat{a}_c \operatorname{sgn}(w). \quad (3)$$

Then, velocity error, e_w , and Coulomb friction parameter error, e_a , can be defined as

$$e_w = w - \hat{w}, \quad (4)$$

$$e_a = a_c - \hat{a}_c. \quad (5)$$

By using (1) (2), we obtain

$$J\dot{e}_w = -J\hat{a}_c \operatorname{sgn}(w) - KJ\dot{e}_w. \quad (6)$$

Then, let us define the following Lyapunov function V , which will also be used in the stability analysis later.

$$V = \frac{1}{2}e_w^2 + \frac{L_1}{2}e_a^2, \quad (7)$$

where $L_1 > 0$ is another observer gain. By taking the derivative of (7) and using (6), we obtain:

$$\dot{V} = e_w \dot{e}_w + L_1 e_a \dot{e}_a \quad (8)$$

$$= -e_w \hat{a}_c \operatorname{sgn}(w) + L_1 e_a \dot{e}_a - K e_w^2. \quad (9)$$

If we choose the following adaptive law

$$\dot{e}_a = \frac{1}{L_1} e_w \operatorname{sgn}(w). \quad (10)$$

Then, (9) becomes

$$\dot{V} = -K e_w^2 \leq 0, \quad (11)$$

which proves that the error system given by (6) and (10) is stable. For time-invariant systems, using LaSalle's Invariance Principle, one could prove asymptotic and even exponential stability (Khalil, 2002). However, due to the term $\operatorname{sgn}(w) \in \{-1, 1\}$, the error system is time-varying and LaSalle's argument cannot be applied directly (J. P. Hespanha, 2004; Khalil, 2002). Moreover, the error system can be viewed as a switching system and in general, the stability properties may depend on the so-called dwell time (J. Hespanha & Morse, 1999; Koru et al., 2018). We will address these issues in the sequel. Assuming that a_c is constant, (10) results in the following adaptive parameter update rule

$$\dot{\hat{a}}_c = -L e_w \operatorname{sgn}(w), \quad (12)$$

where $L = 1/L_1 > 0$. Using (6) and (12) state space representation of error vector $e = [e_w \ e_a]^T$ can be obtained as Odabaş (2021)

$$\frac{d}{dt} \begin{bmatrix} e_w \\ e_a \end{bmatrix} = \underbrace{\begin{bmatrix} -K & -\operatorname{sgn}(w) \\ L \operatorname{sgn}(w) & 0 \end{bmatrix}}_{A(w)} \begin{bmatrix} e_w \\ e_a \end{bmatrix}. \quad (13)$$

Note that the sign of off-diagonal terms in $A(w)$ changes according to the sign of velocity. In this manner, $A(w)$ can be treated as a system switching between $A_1(w)$ and $A_2(w)$ based on velocity

signs. To clarify, $A_1(w)$ is associated with $w \geq 0$ while $A_2(w)$ is associated $w < 0$. Then, under this statement, they become

$$A_1(w) = \begin{bmatrix} -K & -1 \\ L & 0 \end{bmatrix}, \quad A_2(w) = \begin{bmatrix} -K & 1 \\ -L & 0 \end{bmatrix}. \quad (14)$$

With the notation given above, we can rewrite the error equation given by (13) as follows:

$$\dot{e} = A(w)e, \quad (15)$$

where $A(w)$ is given by (13). Note that $A(w) = A_1$ when $w \geq 0$ and $A(w) = A_2$ when $w < 0$ as given by (14).

2.2 Stability analysis of the observer

As stated above, (11) proves the stability of the new observer, but not necessarily the asymptotic stability due to the switching nature of the whole system. The fundamental underlying reason is that LaSalle's Invariance Theorem is not directly applicable to our case due to the time-varying behaviour of the switching signal. Nevertheless, depending on some assumptions on the switching systems, asymptotic stability results could be obtained without utilising LaSalle's Invariance (J. P. Hespanha, 2004). This requires that the switching signal have certain properties, depending on the so-called dwell-time. We will follow the methodology and results given in J. P. Hespanha (2004) in the sequel. To adopt the notation of J. P. Hespanha (2004), we first define the following quantities. Let $\sigma(\cdot) : [0, \infty) \rightarrow \Sigma_2 = \{1, 2\}$ be a piecewise continuous function. Note that we will also refer to $\sigma(\cdot)$ as the switching function. In our case, $\sigma(t)$ will depend on the sign of $w(t)$; i.e.

$$\sigma(t) = \begin{cases} 1, & w(t) \geq 0, \\ 2, & w(t) < 0. \end{cases} \quad (16)$$

By using (16) we can rewrite (15) in the following form:

$$\dot{e} = A_{\sigma(t)} e \quad (17)$$

Since $\sigma(\cdot)$ is piecewise continuous, there exists a sequence $\{t_k \mid k = 0, 1, \dots\}$ such that $t_{k+1} > t_k$ and $t_k \rightarrow \infty$ as $k \rightarrow \infty$. For simplicity, one may assume $t_0 = 0$. In our case, the instance t_k will denote the times that $w(t)$ changes the sign.

From a mathematical point of view, $\sigma(t)$ could be arbitrary, but if it has certain regularity, it was shown in J. P. Hespanha (2004) that one can prove asymptotic stability by using rather general results. Next, we will give these regularity conditions.

We assume that $\sigma(t)$ satisfies the following properties:

- (A1) $\sigma(t) \in \Sigma_2$ and constant for $t_k < t < t_{k+1}$, $\forall k$.
- (A2) For any t and τ such that $t_k < t < t_{k+1} < \tau < t_{k+2}$, $\sigma(t) \neq \sigma(\tau)$, $\forall k$.
- (A3) There exists a $\tau_D > 0$ such that $t_{k+1} - t_k \geq \tau_D$, $\forall k$.

Now, maximum $\tau_D > 0$ satisfying A3 is called dwell-time of the switching signal. Note that (7) could be written as follows

$$V = \frac{1}{2}e_w^2 + \frac{1}{2}L_1e_a^2 = \frac{1}{2} \begin{bmatrix} e_w & e_a \end{bmatrix} \begin{bmatrix} 1 & 0 \\ 0 & L_1 \end{bmatrix} \begin{bmatrix} e_w \\ e_a \end{bmatrix}. \quad (18)$$

Let us define the symmetric positive definite matrix P as

$$P = \begin{bmatrix} 1 & 0 \\ 0 & L_1 \end{bmatrix}. \quad (19)$$

Note that we can rewrite (18) as

$$V = \frac{1}{2}e^T P e. \quad (20)$$

Clearly, by using (11), (13) and (14) we obtain

$$A_i^T P + P A_i = - \begin{bmatrix} 2K & 0 \\ 0 & 0 \end{bmatrix}, \quad i = 1, 2. \quad (21)$$

Next we define C_1 and C_2 as follows:

$$C_1 = C_2 = \begin{bmatrix} \sqrt{2K} & 0 \end{bmatrix}. \quad (22)$$

From (21), it easily follows that

$$A_i^T P + P A_i = -C_i^T C_i, \quad i = 1, 2. \quad (23)$$

Moreover, the pairs (C_i, A_i) are observable, $i = 1, 2$. Now let us define $C = C_1 = C_2$ and y as follows

$$y = C e. \quad (24)$$

At this point by using (13)–(17) we can obtain some simple results. To be precise, let $\tau \geq 0$, $e(\tau) \in \mathbb{R}^2$, the switching signal $\sigma(\cdot)$, the switching instances $\{t_k | k = 0, 1, \dots\}$ be given and assume that the assumptions A1–A3 are satisfied. Furthermore, assume that $t_i < \tau < t_{i+1} < t_{i+2} < \dots$ holds, and thus we have $\sigma(t) = \sigma(t_k)$ for $t \in [t_k, t_{k+1}]$. Then, the solution of (17) is given as

$$e(t) = e^{A_{\sigma(t_i)}(t-\tau)} e(\tau), \quad t \in [\tau, t_{i+1}) \quad (25)$$

and

$$e(t) = e^{A_{\sigma(t_{i+1})}(t-t_{i+1})} e^{A_{\sigma(t_i)}(t_{i+1}-\tau)} e(\tau), \quad t \in [t_{i+1}, t_{i+2}). \quad (26)$$

This easily follows since error Equation (17) becomes $\dot{e} = A_{\sigma(t_i)} e$ for $t \in [\tau, t_{i+1})$ and $\dot{e} = A_{\sigma(t_{i+1})} e$ for $t \in [t_{i+1}, t_{i+2})$. This approach could be extended to arbitrary $t \geq \tau$. More precisely, under the conditions stated above. Assume that we have $t_i \leq \tau < t_{i+1} < \dots < t_k \leq t < t_{k+1}$. Then the solution of (17) can be given as

$$e(t) = e^{A_{\sigma(t_k)}(t-t_k)} e^{A_{\sigma(t_{k-1})}(t_k-t_{k-1})} \dots e^{A_{\sigma(t_i)}(t_{i+1}-\tau)} e(\tau), \quad t \in [t_{i+1}, t_{i+2}). \quad (27)$$

For future reference, (27) could be written as

$$e(t) = \phi(t, \tau) e(\tau) \quad (28)$$

where the state transition function $\phi(t, \tau)$ is given as

$$\phi(t, \tau) = e^{A_{\sigma(t_k)}(t-t_k)} \dots e^{A_{\sigma(t_i)}(t_{i+1}-\tau)}. \quad (29)$$

See e.g. Section 2.3, Sun and Ge (2011). These results could be summarised as follows:

Proposition 2.1: Let $\tau \geq 0$, $e(\tau) \in \mathbb{R}^2$, the switching signal $w(\cdot)$ be given and assume that the assumptions A1–A3 are satisfied. Then, the error system given by (17) has a unique and continuous solution for $t \geq \tau$. Moreover, $e(\cdot)$ is differentiable except at the switching instances.

Proof: The result easily follows from the developments presented above and (27). ■

Note that Proposition 2.1 can easily be proven using classical results on differential equations. To see that let $w(\cdot)$ be given, assume that the switching function $\sigma(t)$ given by (16) satisfies A1–A3 and define $f(t, e) = A(w)e$. Clearly, f is piecewise continuous in t and globally Lipschitz in e . Then the Proposition 2.1 follows from classical theorems on differential equations, see e.g. Theorem 3.2, Khalil (2002). However, the explicit formulation given by (27)–(29) has other important consequences. Note that in our case $\sigma(t) \in \{1, 2\}$, hence $A_{\sigma(t)} \in \{A_1, A_2\}$. Since A_1 and A_2 are stable matrices by construction, we have constants $M \geq 1$ and $\delta > 0$ such that the following holds

$$\|e^{A_i t}\| \leq M e^{-\delta t}, \quad \forall t \geq 0. \quad (30)$$

If the switching signal $w(\cdot)$ satisfies A3, then we have

$$\|e^{A_{\sigma(t_i)}(t_{i+1}-t_i)}\| \leq M e^{-\delta \tau_D}. \quad (31)$$

Clearly if the following holds:

$$\tau_D > \frac{\ln M}{\delta}, \quad (32)$$

then we have $M e^{-\delta \tau_D} < 1$. This shows that each exponent in (27) becomes a contraction if τ_D is sufficiently large. This leads us to the following well known result.

Proposition 2.2: Under the conditions stated in Proposition 2.1, the solutions of (17) are asymptotically stable provided that the dwell-time τ_D given in A3 is sufficiently large.

Proof: The proof of this well-known fact follows easily from (27)–(32). Note that, in this case, the decay is actually exponential, which easily follows from (31), (32) and (27). ■

Note that Proposition 2.2 is a consequence of what is called as dwell-time stability, see e.g. Section 1.2.2 in Sun and Ge (2011), Lemma 2 in Morse (1996). Note that the results given so far are related to general properties of linear switching systems under the assumptions A1–A3, and we have not utilised the existence of a common Lyapunov function given by (7) which results in (11). In this case, we can have a stronger result, which is valid for all $\tau_D > 0$.

Proposition 2.3: Under the conditions stated in Proposition 2.1, the signal $y(\cdot)$ given by (24) is continuous; moreover, $y \in \mathbf{L}_2$ and $y(t) \rightarrow 0$ as $t \rightarrow \infty$.

Proof: Since $e(\cdot)$ is continuous by Proposition 2.1, so is $y(\cdot)$, see (24). From (11), (20) and (24) we obtain

$$\dot{V} = -Ke_w^2 = -\frac{1}{2}(Ce)^T(Ce) = -\frac{1}{2}y^2. \quad (33)$$

By integrating (33) we obtain

$$\int y^2(s)ds = 2V(0) - 2V(t) \leq 2V(0), \quad \forall t \geq 0. \quad (34)$$

It follows from (34) that $y \in \mathbf{L}_2$. Since \dot{y} is bounded wherever it exists, by Barbalat's Lemma it follows that $y(t) \rightarrow 0$ as $t \rightarrow \infty$, see e.g. Khalil (2002). ■

Remark 2.1: We need to clarify certain points. Let $e = [e_w e_a]^T \in \mathbf{R}_2$ be the error given by (15) since e_w is the velocity estimation error and e_a is the friction parameter estimation error. Proposition 2.2 shows that, under the conditions stated in Proposition 2.1, the error vector $e(t)$ is asymptotically stable, i.e. $e(t) \rightarrow 0$ as $t \rightarrow \infty$ provided that the dwell-time τ_D is sufficiently large, see (32). This result is rather general and does not require the existence of a common Lyapunov function. However, the error system given by (15) has a common Lyapunov function as given by (7), which results in (11), and by using this we can assert stability of the error system, i.e. $e(t)$ is bounded independent of $\tau_D > 0$. Note that if the system given by (15) were the time-invariant, after (11), we could directly conclude that $e_w(t) \rightarrow 0$ as $t \rightarrow \infty$ and that all solutions converge to the largest invariant set inside the set $\mathcal{S} = \{e \in \mathbf{R}^2 \mid \dot{V} = 0\}$ by LaSalle's Invariance Principle. However, (15) is a time-varying system and hence we cannot use LaSalle's Invariance to prove the stability, see e.g. Khalil (2002), as indicated before. Nevertheless, by using Barbalat's Lemma, Proposition 2.1 and (11), we can prove that $e_w \rightarrow 0$ as $t \rightarrow \infty$. This result is valid for arbitrary $\tau_D > 0$. Note that at this point we cannot conclude that $e_a \rightarrow 0$ as $t \rightarrow \infty$. In the sequel, we show that in addition to having a common Lyapunov function, if we further assume that the error system given by (15) with the output defined as e_w satisfies certain observability conditions, one can also prove that $e_a(t) \rightarrow 0$ as well. This will be shown in the sequel.

Next we will show that under certain conditions we have $e_a(t) \rightarrow 0$ in (15) as well. To prove this result, we first need the following technical lemma.

Lemma 2.1: Let $A \in \mathbf{R}^{2 \times 2}$ and $C \in \mathbf{R}^{1 \times 2}$ be given, and assume that the pair (A, C) is observable. There exists an $M > 0$ such that for any $\lambda > 0$, one can find a vector $L \in \mathbf{R}^{2 \times 1}$ such that the following holds:

$$\|e^{(A+LC)t}\| \leq M\lambda^2 e^{-\lambda t}, \quad \forall t \geq 0. \quad (35)$$

Proof: See Lemma 3.2 of Cheng et al. (2005). A systematic way of finding such a $L \in \mathbf{R}^{2 \times 1}$ is also given in Cheng et al. (2004). The constant $M > 0$ is related to the transformation matrix which transforms (A, C) to observable canonical form and hence is independent of $L \in \mathbf{R}^{2 \times 1}$. The special form of the right-hand side of (35) is related to a special eigenvalue assignment related to a Vandermonde matrix. ■

We note that a similar result is also given in Pait and Morse (1994) and J. P. Hespanha (2004). A direct consequence of Lemma 2.1 is the following result:

Corollary 2.1: Consider the matrices A_1 and A_2 given by (14). Assume that $K > 0$ and $L > 0$ are given. Then, there exists an $M > 0$ such that for any $\lambda > 0$, one can find vectors $L_1, L_2 \in \mathbf{R}^{2 \times 1}$ such that the following holds,

$$\|e^{(A_i+L_i C)t}\| \leq M\lambda^2 e^{-\lambda t}, \quad \forall t \geq 0. \quad (36)$$

where $C \in \mathbf{R}^{1 \times 2}$ is given by (22), (24).

Proof: Since (A_i, C) is observable for $i = 1, 2$, this result trivially follows from Lemma 2.1. ■

Before we state our main stability result, we first point out the following trivial fact.

Fact 2.1: Let $A, B \in \mathbf{R}^{n \times n}$ be given and consider the following equations:

$$\dot{x} = Ax, \quad (37)$$

$$\dot{z} = Az + Bz - Bz. \quad (38)$$

Let $x(0) = z(0) := x_0 \in \mathbf{R}^n$ be given and let $x(t)$ and $z(t)$ be the solutions of (37) and (38), respectively. Then, $x(t) = z(t) \forall t$.

Proof: Since both equations are linear, they have unique solutions $x(t)$ and $z(t)$, for $\forall t \geq 0$. Hence, $Bz(t)$ is finite $\forall t \geq 0$. Therefore, $Bz(t) - Bz(t) = 0 \forall t \geq 0$. Hence, (37) and (38) represent the same differential equation. Therefore, $x(t) = z(t) \forall t$. ■

Remark 2.2: Note that (37) and (38) are exactly the same equation and (38) is not a transformed form of (37). Also, note that the solutions of (37) and (38) can be given as follows:

$$x(t) = e^{At}x_0, \quad (39)$$

$$z(t) = e^{(A+B)t}x_0 - \int_0^t e^{(A+B)(t-\tau)}z(\tau)d\tau. \quad (40)$$

Note that by Fact 2.1, we have $x(t) = z(t), \forall t \geq 0$. This may not be immediately seen from (39) and (40). However, it could be proven in various ways. The simplest way to see this is to use Laplace transform in (40), which leads:

$$Z(s) = (sI - A - B)^{-1}x_0 - (sI - A - B)^{-1}BZ(s). \quad (41)$$

By multiplying both sides with $(sI - A - B)$, and cancelling $BZ(s)$ terms, we obtain

$$(sI - A)Z(s) = x_0 \quad (42)$$

which leads to $Z(s) = (sI - A)^{-1}x_0$, and hence $z(t) = e^{At}x_0$. Since $x(t) = e^{At}x_0$, we have $x(t) = z(t) \forall t \geq 0$.

The result given in Fact 2.1 trivially extends to the switching case. More precisely, we have the following:

Corollary 2.2: Consider the system given by (17). Let the switching signal $w(t)$, switching instances $\{t_k | k = 0, 1, \dots\}$, and the switching function $\sigma(t)$ be given as in (16) and assume that A1–A3 are satisfied. For any given $B_1, B_2 \in \mathbf{R}^{2 \times 2}$, let us define $B_{\sigma(t)}$ accordingly, see (16), and consider the following equation:

$$\dot{z} = A_{\sigma(t)}z + B_{\sigma(t)}z - B_{\sigma(t)}z. \quad (43)$$

Then, for any $e_0 \in \mathbf{R}^2$ and $\tau \geq 0$, the solution $e(t)$ of (17) and $z(t)$ of (43) with $e(\tau) = z(\tau) = e_0$ for $t \geq \tau$ satisfies $e(t) = z(t) \forall t \geq \tau$.

Proof: Note that the right-hand side of (43) is either $A_1z + B_1z - B_1z$ or $A_2z + B_2z - B_2z$, due to switching. Then, the result trivially follows from Proposition 2.2 and Fact 2.1. ■

Based on the developments given above, we now state our next stability result.

Proposition 2.4: Let $\tau \geq 0$, $e(\tau) = e_0 \in \mathbf{R}^2$, the switching signal $w(t)$, switching instances $\{t_k | k = 0, 1, \dots\}$, the switching function $\sigma(t)$ (see (16)) be given and assume that the assumptions A1–A3 are satisfied. Furthermore, assume that $\sigma(t) = \sigma(t_k)$, $t \in [t_k, t_{k+1})$ and $t_i \leq \tau < t_{i+1} < t_{i+2}$ holds. For any given $L_1, L_2 \in \mathbf{R}^{2 \times 1}$, define $L_{\sigma(t)}$, accordingly, see (16). Let $e(t)$ be the solution of (15), or equivalently of (17) for $t \geq \tau$. Then, the following statements hold.

(i) Consider the following system

$$\dot{z} = A_{\sigma(t)}z + L_{\sigma(t)}Cz - L_{\sigma(t)}Cz. \quad (44)$$

Let $z(t)$ be the solution of (44) for $z(\tau) = e(\tau) = e_0$ for $t \geq \tau$. Then, $z(t) = e(t) \forall t \geq \tau$

(ii) Let L_1 and L_2 be chosen appropriately according to Corollary 2.2 so that the state transition matrix $\phi(t, \tau)$ of the operator $A_{\sigma(t)} + L_{\sigma(t)}C$ is exponentially stable. Then $z(t) \rightarrow 0$ as $t \rightarrow \infty$ (hence $e(t) \rightarrow 0$ as $t \rightarrow \infty$).

Proof: Part i, trivially follows from Corollary 2.2. For part ii, note that by using the state transition function $\phi(t, \tau)$ of the operator $A_{\sigma(t)} + L_{\sigma(t)}C$, the solution $z(t)$ of (44) is given as

$$z(t) = \phi(t, \tau)e(\tau) - \int_{\tau}^t \phi(t, s)L_{\sigma(s)}Cz(s)ds \quad (45)$$

see (40) and Remark 2.2. Note that (45) holds for any $L_{\sigma(t)}$, and trivially follows from Corollary 2.2, see Remark 2.2. Moreover, by part i, $z(t) = e(t) \forall t \geq \tau$. Hence by (24), $Cz(t) = y(t) \forall t$, and by Proposition 2.3, we have $Cz(t) \in \mathbf{L}_2$. If $\phi(t, \tau)$ is exponentially stable, then the first term in the right hand side of (45) decays to zero. The second term in the right hand side of (45) is the convolution of an exponentially stable kernel with an \mathbf{L}_2 function. By standard results it can be easily shown that this term decays to zero as well, see e.g. Theorem 1 in Section 6.4 of Vidyasagar (1978), or the proof of Theorem 4 of J. P. Hespanha (2004). ■

The stability result given in part ii of Proposition 2.4 will be complete if one can show that there exists matrices L_1

and L_2 such that the state transition matrix $\phi(t, \tau)$ of the operator $A_{\sigma(t)} + L_{\sigma(t)}C$ is exponentially stable. This follows from Corollary 2.1 since (A_i, C) are observable. This proof is not induced in Proposition 2.4 to improve the readability. The next result clarifies this point.

Lemma 2.2: Assume that the conditions stated in Proposition 2.4 holds. Then, there exists vectors $L_1, L_2 \in \mathbf{R}^{2 \times 1}$ such that the state transition function $\phi(t, \tau)$ of the operator $A_{\sigma(t)} + L_{\sigma(t)}C$ is exponentially stable, where $\sigma(t)$ is given as in (16) and $L_{\sigma(t)}$ is defined accordingly.

Proof: This result easily follows from Lemma 2.1 and Proposition 2.1. Note that the expression of $\phi(t, \tau)$ is similar to (39); more precisely, we have the following:

$$\phi(t, \tau) = e^{(A_{\sigma(t_k)} + L_{\sigma(t_k)}C)(t-t_k)} \dots e^{(A_{\sigma(t_i)} + L_{\sigma(t_i)}C)(t_{i+1}-\tau)} \quad (46)$$

If L_1 and L_2 are chosen according to Corollary 2.2, by using (46), we obtain the following

$$\|e^{(A_{\sigma(t_j)} + L_{\sigma(t_j)}C)(t_{j+1}-t_j)}\| \leq M\lambda^2 e^{-\lambda(t_{j+1}-t_j)} \quad (47)$$

where $j = 2, 3, \dots, k-1$. By assumption 3, we have $t_{j+1} - t_j \geq \tau_D$, and hence from (36) we have

$$\|e^{(A_{\sigma(t_j)} + L_{\sigma(t_j)}C)(t_{j+1}-t_j)}\| \leq M\lambda^2 e^{-\lambda\tau_D}. \quad (48)$$

Hence, if the following holds

$$\tau_D > \frac{\ln(M\lambda^2)}{\lambda}, \quad (49)$$

then each term in (46) becomes contraction, cf. (30), (32). Therefore, if (49) holds, then $\phi(t, \tau)$ becomes contraction and $\phi(t, \tau) \rightarrow 0$ as $t \rightarrow \infty$. That the decay is exponential can be proven easily by stated results, see the arguments following the proof of Proposition 2.2. Since M is a constant and $\lambda > 0$ can be chosen arbitrarily for any $\tau_D > 0$, one can choose $\lambda > 0$ so that (49) is satisfied, and find the gains L_1 and L_2 according to Corollary 2.1. This concludes the proof. ■

A consequence of Lemma 2.2 is the following result:

Corollary 2.3: Under the conditions stated in Proposition 2.4, error system given by (24) is exponentially stable, i.e. for any given $\tau \geq 0$ and $e(\tau) \in \mathbf{R}^2$, the following holds for some $C \geq 1$ and $\mu > 0$:

$$\|e(t)\| \leq Ce^{-\mu(t-\tau)}\|e(\tau)\|, \quad \forall t \geq \tau. \quad (50)$$

Proof: This follows from a more general result on the equivalence of uniform asymptotic stability and exponential stability, see e.g. Theorem 2 of Angeli et al. (2009), Theorem 4 of J. P. Hespanha (2004). ■

Now, several remarks are in order.

Remark 2.3: It would be interesting to comment on the decay rate $\mu > 0$ indicated in (50). From (45), we easily assume that μ might be related to the state transition function $\phi(t, \tau)$ of the

operator $A_{\sigma(t)} + L_{\sigma(t)}C$, which is given by (46). To investigate further, let us assume that in the interval $[\tau, t)$ we have total k switchings. Then, from (46), we obtain

$$\|\phi(t, \tau)\| \leq (M\lambda^2)^{k+1} e^{-\lambda(t-\tau)}. \quad (51)$$

By assumption A3, we have $t_{j+1} - t_j \geq \tau$, hence we have:

$$t - \tau \geq (k - 1)\tau_D \quad (52)$$

which implies

$$k \leq \frac{t - \tau}{\tau_D} + 1. \quad (53)$$

By using (53) in (52) we obtain:

$$\|\phi(t, \tau)\| \leq \hat{C}e^{-\hat{\mu}(t-\tau)}. \quad (54)$$

where $\hat{C} = (M\lambda^2)^2$ and $\hat{\mu}$ is given by

$$\hat{\mu} = \lambda - \frac{\ln(M\lambda^2)}{\tau_D}. \quad (55)$$

Clearly, $\hat{\mu} > 0$ if and only if (49) holds. Note that $\hat{\mu}$ is an estimation of the decay rate for the operator $A_{\sigma(t)} + L_{\sigma(t)}C$. By using this, the decay rate for the error system given by (15) or equivalently by (17), could be obtained from (45). Nevertheless from (49) and (55), we may deduce that the actual decay rate depends on the dwell time $\tau_D > 0$ in a complicated way. The actual relation between these terms deserves and requires further investigation. Also both (49) and (55) indicate that for the stability analysis presented here, we need $\tau_D > 0$. Since $t_{k+1} - t_k \geq \tau_D$, this condition implies that the switching frequency is finite. If this condition fails, e.g. when $t_{k+1} - t_k \rightarrow 0$ as $k \rightarrow \infty$, the asymptotic stability results provided here may not hold.

Remark 2.4: Note that the error system given by (15), or equivalently by (17), is a time-varying system. Hence, the classical LaSalle's Invariance Principle cannot be applied. This point was mentioned in Remark 2.1. Our first stability result is given by Proposition 2.1 indicates that if the dwell time τ_D is sufficiently large the error given by (15) is exponentially stable. This is rather general and well known and is referred to as dwell-time stability, see e.g. Section 1.2.2 in Sun and Ge (2011). When (i): the switching system has a common Lyapunov function, see (7) or (20), (ii): the derivative of this function is negative-definite which depends on the error signal in a linear way, see (11) and (24) and (iii): a certain observability condition is satisfied, see (23) and (24), then we can prove asymptotic stability of the error system given by (15) provided that the switching signal has finite frequency, i.e. $\tau_D > 0$. Note that in none of these stability proofs, we utilise LaSalle's Invariance Principle, implicitly or explicitly. In proving latter instead of (15) or (17), we add and subtract the same term in these equations and obtain the same system in a different form, see (38), (43). Note that this is not a transformation but exactly as same as the original system given by (15), or equivalently (17).

Remark 2.5: We note that the essential part in the regularity conditions is the assumption that $t_{k+1} - t_k \geq \tau_D$. This implies

that the switching frequency is finite. To demonstrate that this condition is essential, in J. P. Hespanha (2004) a switching system which is essentially the same as given by (14) is considered, and a special switching sequence for which $t_{k+1} - t_k \approx o(1/k)$ is constructed and it was shown that the system remains stable, but asymptotic stability does not hold. Note that for such a switching signal, the condition A3 is not satisfied, i.e. this switching signal does not have a nonzero dwell-time, and as a result, switching frequency does not remain finite.

Remark 2.6: Indeed, there are plenty of adaptive observer designs in the literature. All of these designs are based on some assumptions and constraints. For instance, [1,2] remarks on such requirements for the well-known Friedland-Park observer's performance and stability. By revisiting these references, the general form of Friedland-Park observer can be acquired as

$$\dot{z} = g'(w(t)) \frac{u}{J}, \quad (56)$$

$$\hat{a}_c = z - g(w(t)). \quad (57)$$

where z and $g(w(t))$ are an internal observer state and the estimation function respectively. Since a_c is a constant, $\dot{a}_c = 0$; therefore, one can obtain friction error dynamics for such an observer as follow

$$\dot{e}_a = -\dot{\hat{a}}_c \quad (58)$$

$$= -g'(w(t)) \operatorname{sgn}(w)e_a. \quad (59)$$

Obviously, under some conditions, one can show the asymptotic stability of the error dynamics given by (58). Indeed, there is a quite large class of functions $g(w)$ satisfying these conditions, although the original Friedland-Park observer utilises $w = k|w|^\mu$ where k and μ are positive design parameters (Odabaş, 2021). To this end, $g(w)$ should belong to a certain Cartesian axis sector.

Consider a function $h : \mathbf{R} \rightarrow \mathbf{R}$ which satisfies the following condition

$$\alpha w^2 \leq wh(w) \leq \beta w^2, \quad \forall w. \quad (60)$$

where $\beta \geq \alpha$. Such functions have a graph in Cartesian axes whose boundaries are given by the lines $y = \alpha w$ and $y = \beta w$ and we say in such a case that $h(\cdot)$ belongs to a sector $[\alpha, \beta]$, or simply $h \in [\alpha, \beta]$, see Khalil (2002) for more details. Particularly, for $\alpha = 0, \beta = \infty, h \in [0, \infty]$ and lies entirely in the first and third quadrants of Cartesian axes.

Under the light of this fact, one can find a differentiable function $g(w) : \mathbf{R} \rightarrow \mathbf{R}$ such that $g'(w(t)) \in [0, \infty)$. In this case, $g'(w)\operatorname{sgn}(w) \geq 0$ since $\operatorname{sgn}(w) \in [0, \infty]$. Furthermore, one can define $G(t) = g'(w(t))\operatorname{sgn}(w(t))$ and assume that there exist some $\theta > 0$ and $T > 0$ such that the following holds

$$\int_t^{t+T} G(s) ds \geq \theta, \quad \forall t \geq 0. \quad (61)$$

Then, asymptotic stability is achieved as $t \rightarrow \infty$. Hence, in Friedland-Park type observer designs, it is necessary to satisfy (61) for a sufficiently long period of time to obtain zero

friction error dynamics with an exponential decay (Odabaş, 2021).

Similarly, Remark 2.5 states that the proposed adaptive observer scheme in this paper requires finite velocity switching frequency such that $t_{k+1} - t_k > \tau_D > 0$. These are some mild assumptions and typical in adaptive control theory to guarantee asymptotic stability. Nevertheless, in Friedland-Park type observer schemes, how fast estimation error dynamics converge to zero for determined function $g(w)$ is implicit. Notably, in the original Friedland-Park Observer, $g(w) = k|w|^\mu$ is employed, which yields $g'(w) = k\mu|w|^{\mu-1}\text{sgn}(w) \in [0, \infty]$ for any positive constants k and μ . However, optimal values for these function parameters are ambiguous; therefore, determined heuristically. On the other hand, the proposed observer structure provides a straightforward method to determine the observer parameter considering settling time and overshoot requirements of the friction estimation.

2.3 Observer parameter selection

Calculating the decay rate in switching systems might be challenging since it generally depends on the dwell time, as in Equation (55). Especially, it becomes severe when dwell time is so short. On the other hand, if the dwell time is large enough, the system's settling time may be expected to converge to the theoretical value computed by the system matrices A_1 or A_2 . Although it is worthy of analysing the relationships among the decay rate, settling time and dwell time, it is out of the main scope of this paper.

Note that $A_1(w)$ and $A_2(w)$ have very similar structures. In fact, they share the same eigenvalues since $|sI - A_i(w)| = s^2 + Ks + L$ for $i = 1, 2$. This equation can be linked to the characteristic equation of a second-order system which is $s^2 + 2w_n\zeta s + w_n^2$. Then,

$$L = w_n^2, \quad (62)$$

$$K = 2w_n\zeta. \quad (63)$$

where ζ and w_n stand for damping ratio and natural frequency of second-order system. Moreover, settling time to within 2% desired output, T_s , and percentage overshoot, PO , equations can be rewritten as below adopting the definitions given in Golnaraghi and Kuo (2017). Then, by considering desired settling time and overshoot performance of the observer response, the parameters K and L can be determined as given in the below relations.

$$T_s = -\frac{2 \ln(0.02\sqrt{1-\zeta^2})}{K}, \quad (64)$$

$$PO = 100e^{-K\pi/\sqrt{4L-K^2}}. \quad (65)$$

If $\zeta = 1$, the settling time can be approximated as

$$T_s = \frac{6}{w_n}. \quad (66)$$

Remark 2.7: Note that although $A_1(w)$ and $A_2(w)$ provide the same characteristic equation, (13) represents a switching system. As a result, the error dynamics of the observer have a

time-varying nature. Therefore, settling time and percentage overshoot properties can converge to the theoretical values given by (64)–(66) only if the switching frequency between these two subsystems $A_1(w)$ and $A_2(w)$, so-called dwell-time, is slow enough. In other words, in order to satisfy desired settling time and percentage overshoot criteria, the dwell time should be long enough. Otherwise, one can still obtain a stable observer structure whose setpoint properties deviate from the theoretical values yet are still affected by the design parameters K and L .

3. Position controller design

In this section, we consider the position control of the system given by (1) and assume that a friction estimation \hat{F} , as given by (3) in Section 2.1, is available. Hence, based on this estimation, we choose the control input u as

$$u = \hat{F}(w) + u_p, \quad (67)$$

where u_p is the output of an appropriate controller. By using a PID controller, the closed-loop system can be given as in Figure 1.

PID controllers are very prominent in many control engineering applications. Theoretically, the distinctive effects of proportional, derivative and integral gains are pretty straightforward. Nevertheless, system bandwidth and desired stability margins set some constraints on selecting controller parameters in practice. Moreover, considering desired steady-state and transient responses, one should care about the tradeoff among controller parameters. In this sense, there are various algorithms for manual or auto-tuning PID controllers (Dorf & Bishop, 2008). In this context, to determine optimal PID coefficients, we apply the integral of time multiplied by the absolute error (ITAE) index, which is defined as

$$\text{ITAE} = \int_0^T t|e(t)| dt, \quad (68)$$

where e is the error is the difference between the reference input and the output of closed-loop feedback system. Assume that plant has a velocity to control input transfer function $P(s)$ as

$$P(s) = \frac{1}{Js}, \quad (69)$$

where J is the moment of inertia. Then we can define general form of position controller, $C(s)$ as follows

$$C(s) = K_p + K_d s + \frac{K_i}{s}, \quad (70)$$

where K_p , K_d and K_i are the proportional, derivative and integral gains, respectively. Consequently, using (69) and (70) and assuming that $F = \hat{F}$, i.e. exact friction cancellation is achieved, we can obtain the closed-loop transfer function of the position control system, $T(s)$ as

$$T(s) = \frac{\frac{K_d}{J}s^2 + \frac{K_p}{J}s + \frac{K_i}{J}}{s^3 + \frac{K_d}{J}s^2 + \frac{K_p}{J}s + \frac{K_i}{J}}. \quad (71)$$

Previously, Graham and Lathrop computed optimum coefficients of the characteristic equation of the closed-loop feedback

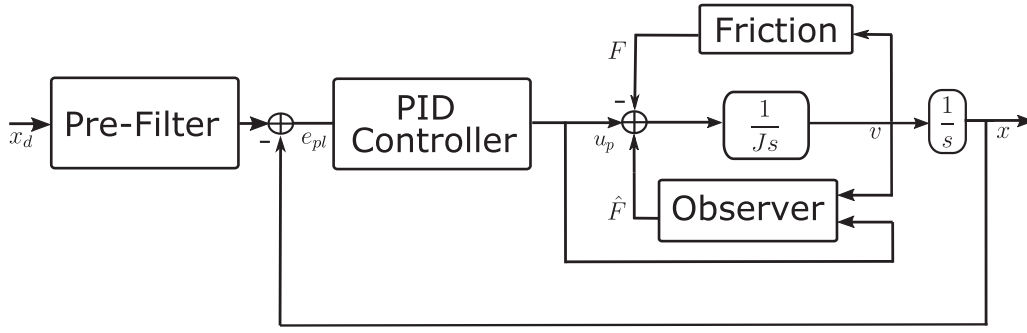


Figure 1. Block diagram of position control system with friction cancellation.

Table 1. Graham and Lathrop derived the set of normalised transfer function coefficients for a step input.

| |
|---|
| $s + w_n$ |
| $s^2 + 1.4w_ns + w_n^2$ |
| $s^3 + 1.75w_ns^2 + 2.15w_n^2s + w_n^3$ |
| $s^4 + 2.1w_ns^3 + 3.4w_n^2s^2 + 2.7w_n^3s + w_n^4$ |
| $s^5 + 2.8w_ns^4 + 5.0w_n^2s^3 + 5.5w_n^3s^2 + 3.4w_n^4s + w_n^5$ |

system by minimising the ITAE criterion when step or ramp input is applied (Graham & Lathrop, 1953). Therefore, it is possible to determine PID parameters considering the bandwidth requirements of the system and (71). For step input tracking, Table 1 presents the optimal coefficients for the transfer functions with different orders. Since the transfer function given in (71) is a third-order function, controller parameters for step input tracking can be revealed as

$$\frac{K_d}{J} = 1.75w_n, \quad \frac{K_p}{J} = 2.15w_n^2, \quad \frac{K_i}{J} = w_n^3. \quad (72)$$

Note that integral gain K_i is proportional to bandwidth cube; as a result, large K_i values may lead to large overshoots. Therefore, as an option, one can employ a pre-filter to mitigate the overshoot. In this case, steady-state performance may also be improved, although settling time is affected negatively. Typically, it is chosen to cancel the fastest negative real axis zero of the closed loop system (Taşdelen & Özbay, 2013). Hence, transfer function $H(s)$ of such filter can be obtained as

$$H(s) = \frac{K_i}{K_d s^2 + K_p s + K_i}. \quad (73)$$

Consequently, the overall position control system can be portrayed as in Figure 1.

4. Simulations

We performed simulations considering a one-degree-of-freedom rotary system without any elastic modes see Baykara (2009). First, we assume that the existing friction includes only the Coulomb coefficient and evaluate the estimation performance of the observer for different parameters. Then, we investigate the observer estimation when the existing friction includes additional LuGre parameters, all presented in Table 2. As previously mentioned, LuGre model is a dynamic friction

Table 2. Parameters used in the simulations.

| Parameter | Notation | Value | Unit |
|-----------------------|------------|-------------------------|-------------------|
| Stribeck velocity | w_s | 0.01 | rad/s |
| Stiffness coefficient | σ_0 | 3.5×10^4 | N.m/rad |
| Damping coefficient | σ_1 | 0.1 | N.m.s/rad |
| Coulomb friction | F_c | 0.285 | N.m |
| Stick friction | F_s | 0.335 | N.m |
| Viscous friction | F_v | 0.018 | N.m.s/rad |
| Total inertia | J | 3.8623×10^{-4} | kg.m ² |

model and it is expressed with the following equations.

$$\frac{dz}{dt} = w - \sigma_0 \frac{|w|}{h(w)} z, \quad (74)$$

$$F(w) = \sigma_0 z + \sigma_1 \frac{dz}{dt} + F_v w. \quad (75)$$

where z is an internal state variable and $h(w)$ is an appropriately chosen function to capture Stribeck effect. Simply it can be determined as

$$h(w) = F_c + (F_s - F_c)e^{-(w/w_s)^2}. \quad (76)$$

Note that for $\frac{dz}{dt} = 0$, the LuGre model given by (74)–(76) reaches steady-state and converges the classical static model described by the following equation.

$$F(w) = [F_c + (F_s - F_c)e^{-(w/w_s)^2}] \text{sgn}(w) + F_v w. \quad (77)$$

In all simulations, we use Runge–Kutta Method with 0.001 ms as a numerical solver and apply a zero mean square wave input with 0.02 rad amplitude and 0.1 Hz frequency in our simulations. Therefore, considering (72) and (73), we obtain the following PID controller and reference filter for $w_n = 62.8$ rad/s.

$$C(s) = 3.28 + 0.04s + \frac{95.66}{s}, \quad (78)$$

$$H(s) = \frac{95.66}{0.04s^2 + 3.28s + 95.66}. \quad (79)$$

As shown in Figure 2, without a friction cancellation, an increasing steady-state error occurs until the direction change. On the other hand, the proposed observer with $K = 72$ and $L = 1296$ eliminates this tracking error. Therefore, although there is an overshoot initially, the closed-loop position feedback system can track the reference input as desired. Note

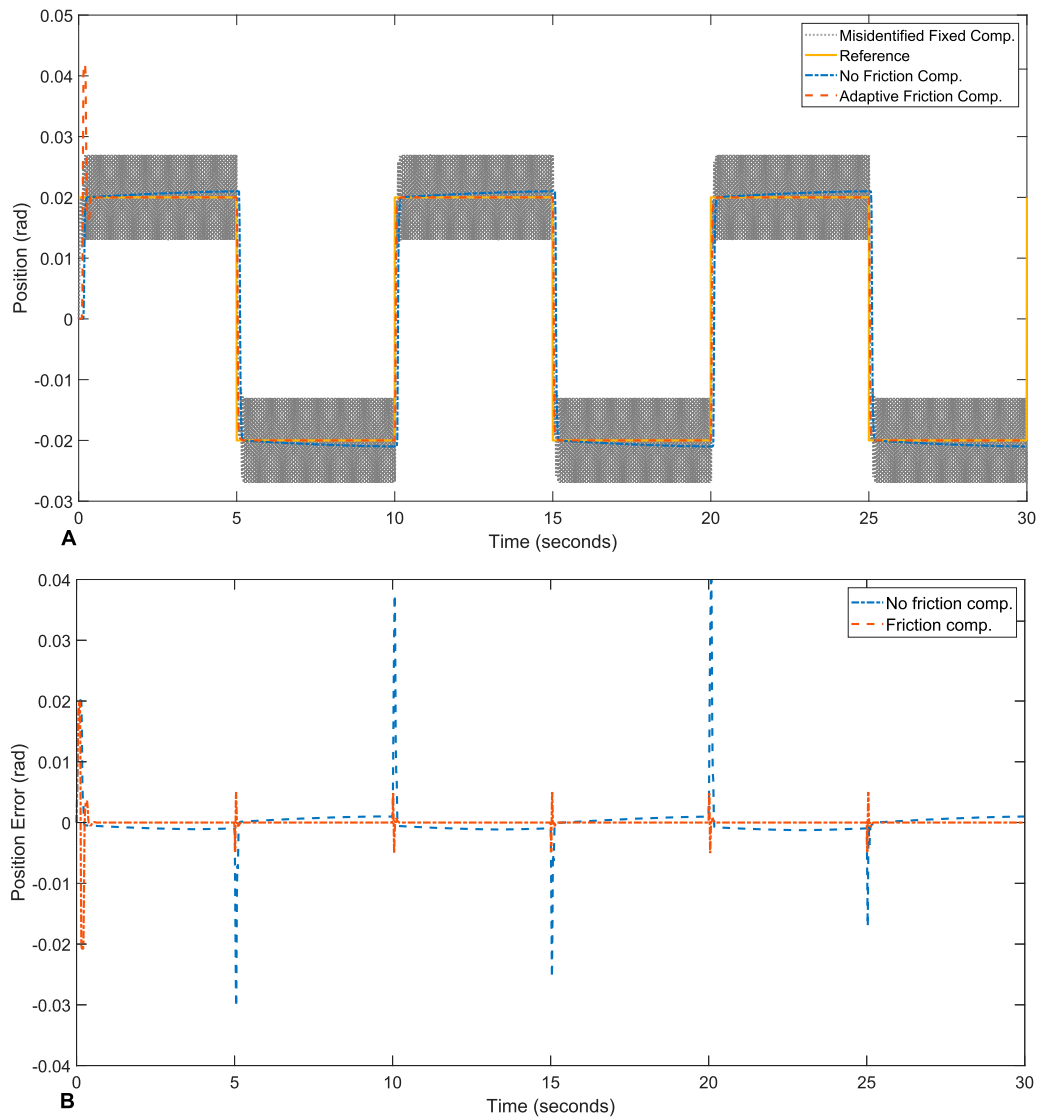


Figure 2. A: Square wave position response of the system under Coulomb Friction Model. B: Position tracking error with and without adaptive friction compensation.

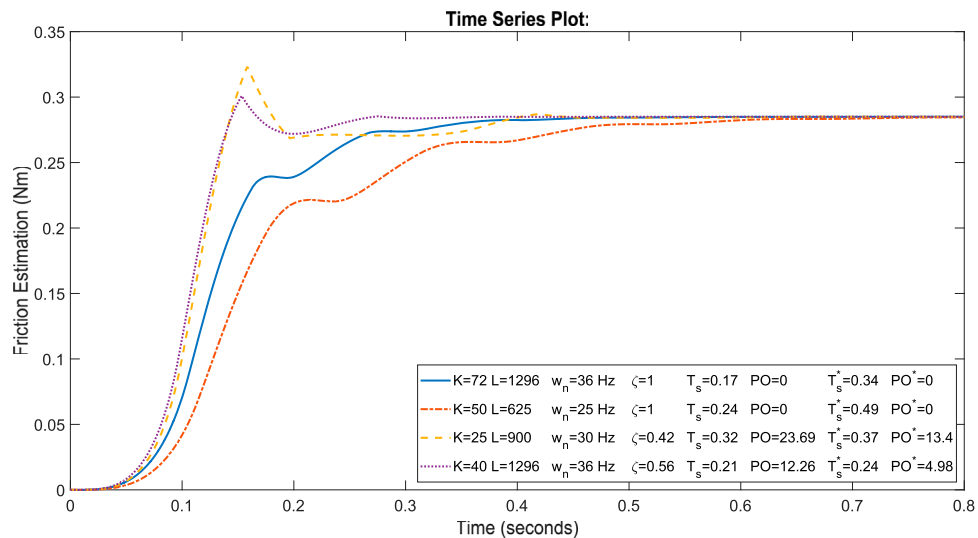


Figure 3. Coulomb friction estimation response of the observer for different design parameters.

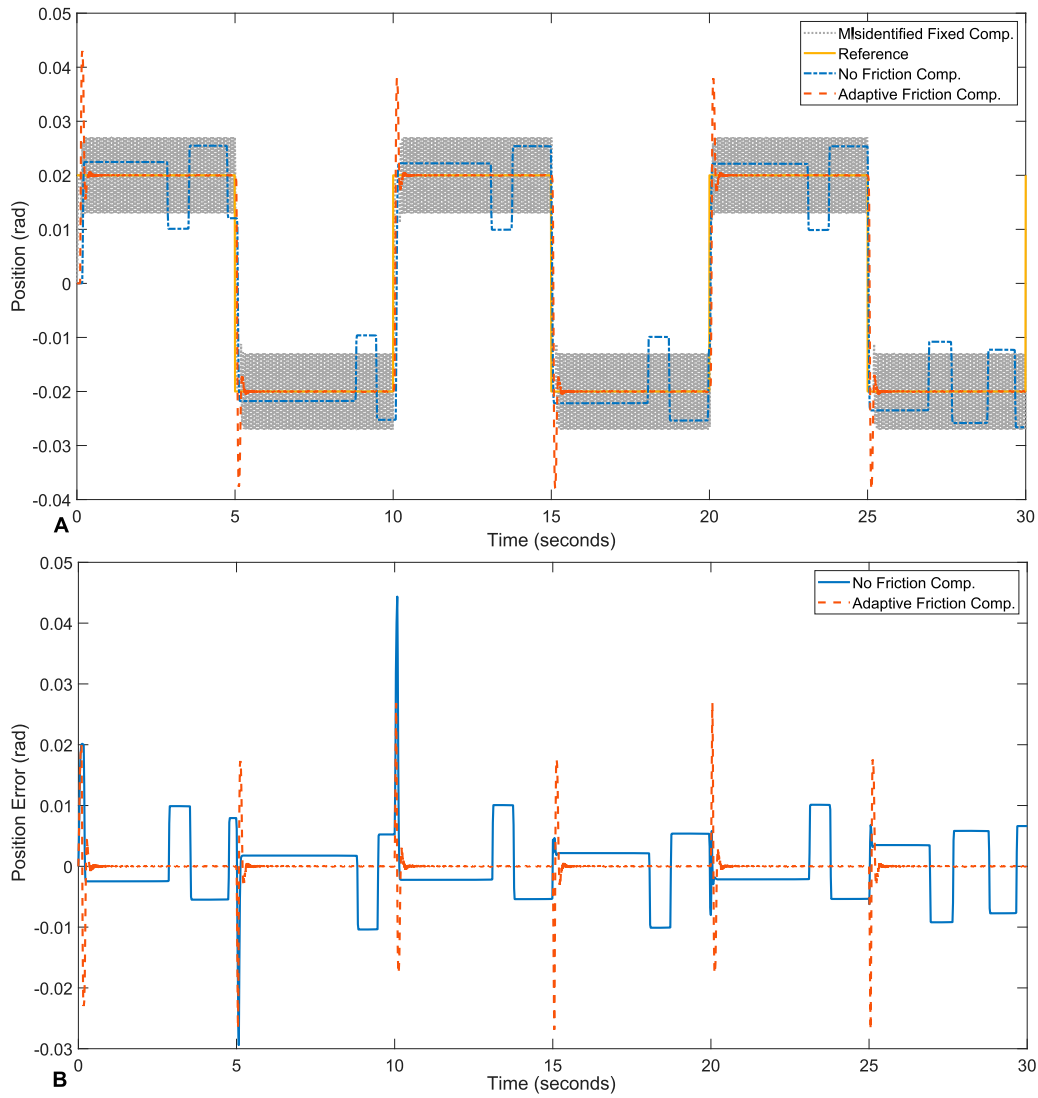


Figure 4. A: Square wave position response of the system under LuGre Friction Model. B: Position tracking error with and without adaptive friction compensation.

that these observer parameters correspond to $\zeta = 1$ and $w_n = 226.19$ rad/s. Hence, according to (65) and (66), percentage overshoot and settling time are approximately equal to 0 and 0.17 s. Furthermore, also we analyse the fixed torque friction compensation with misidentified Coulomb coefficient. To clarify, we assume that there exists a 5% per cent identification error such that $\hat{F}_c = 0.299$. In this case, system performance degrades drastically as shown in Figure 2

What is more, for this system, observer estimation performance is analysed for different design parameters as given in (62)–(66). Nevertheless, in practice, estimation performance may slightly diverge from these theoretical parameters due to the designed controller or employed other structures such as reference filter. In Figure 3, theoretical and acquired estimation performance comparisons for different observer designs are presented. In this analysis, simulated settling time and percentage overshoot results are denoted by T_s^* and PO^* respectively. The difference between theory and practice is mainly due to the switching and hence essentially the time-varying nature of the underlying observer dynamics. As explained Remark 2.7 if the switching becomes less frequent, one expects that these

mismatches may diminish and the second-order approximation becomes more accurate. Notwithstanding, theoretical and practical results exhibit similar trends.

Secondly, we investigate the observer performance again with $K = 72$ and $L = 1296$ when the existing friction possesses LuGre Model characteristics. Similar to the Coulomb Model case, we again analyse the fixed torque friction compensation with misidentified static friction parameters. In this case, a 5% per cent identification error leads to $\hat{F}_c = 0.299$ and $\hat{F}_s = 0.352$ for friction compensation. Once again, chattering is observed in Figure 4. Additionally, without any compensation, the system exhibits a stick-slip behaviour aggravated by the integral component of the controller. This particular behaviour is named hunting in the literature, see Armstrong-Hélouvry et al. (1994). Furthermore, fixed torque compensation with misidentified static friction coefficients results in a chattering behaviour and best tracking performance is achieved while the proposed adaptive observer is employed. In this respect, the contribution of the adaptive observer is incontrovertible.

Lastly, we design another PID controller and reference filter for $w_n = 220$ rad/s to investigate the effect of controller

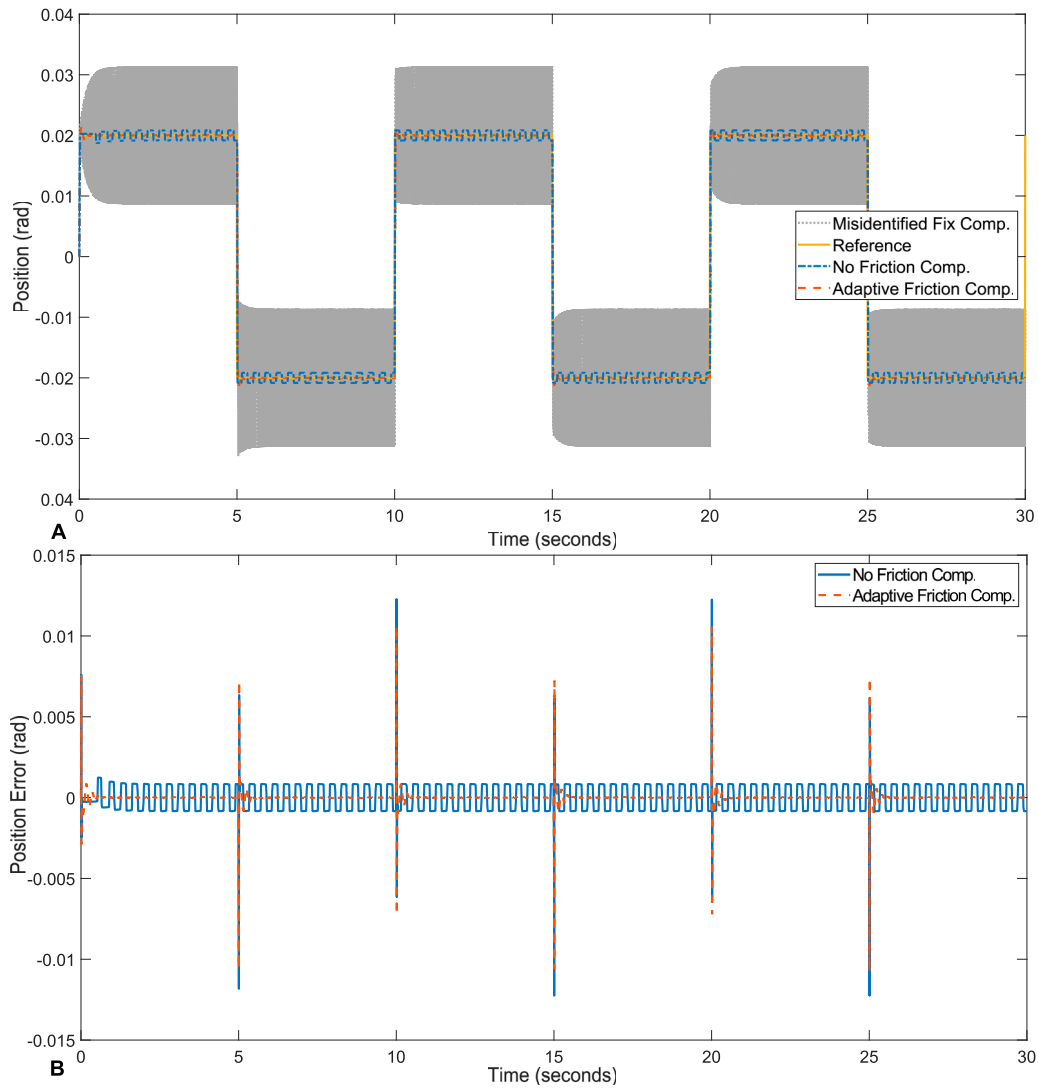


Figure 5. A: Square wave position response of the system under LuGre Friction Model for ITAE index-based PID controller with $w_n = 220$ rad/s. B: Position tracking error with and without adaptive friction compensation.

bandwidth on friction cancellation. In this case corresponding transfer functions become

$$C(s) = 40.16 + 0.15s + \frac{4107.53}{s}, \quad (80)$$

$$H(s) = \frac{4107.53}{0.15s^2 + 40.16s + 4107.53}. \quad (81)$$

From Figure 5, without a friction cancellation, limit cycle behaviour due to hunting diminishes when the controller bandwidth increases. Moreover, in this case, the system can track the desired position input well enough; as a result, the usage of the proposed observer eventually may become redundant for large enough controller bandwidths. Besides, large controller bandwidth may help to reduce the overshoot on the position response at the direction reversals. Nevertheless, the system performance deteriorates when the misidentified fixed torque compensation is applied since the system becomes sensitive to mismatches due to aggressive controller structure.

5. Conclusions

In this work, we proposed a novel friction observer and investigated its stability properties. Then, we applied the proposed friction observer to the position control of a typical second-order system. To this end, we considered the position control performance of a simple mechanical system under static and dynamic friction. In particular, friction cancellation becomes vital when the dynamic LuGre friction model is addressed. Moreover, in this case, precise identification of friction parameters becomes challenging. Therefore, fixed torque compensation with erroneous coefficients may lead to performance degradation due to chattering. In this manner, the proposed adaptive observer improves the tracking significantly.

Furthermore, the design parameters of this structure can be determined considering the overshoot and settling time properties of a second-order system. What is more, it adopts both friction and velocity error dynamics to estimate existing friction in the system that is why it may tolerate uncertainties on velocity measurement. This novel observer design may come into prominence compared to other adaptive observer

schemes with these features. Nevertheless, under the presence of relatively large constant measurement delays, the friction estimation of the presented observer may be hindered due to poor velocity prediction. In this case, a standalone velocity predictor may be required. To this end, Odabaş (2021); Odabaş and Morgül (2020) exhibit several ordinary differential equation solver-based predictors and approximate time delay with invertible rational functions to extinguish the effects of the delay. Note that these predictor schemes assume that measurement delay is fixed and known. When the delay is time-varying or is known with a mismatch, utilising introduced observer design with such a separate velocity predictor still may be advantageous since the observer considers velocity error dynamics as well for friction estimation.

Apparently, without any friction observer, controller bandwidth should be large enough in order to prevent hunting. However, the larger controller bandwidth implies the larger PID coefficients, which may not always be possible due to design constraints or sensitivity concerns to nonlinearities within the system. Therefore, the contribution of the adaptive observer to the tracking performance becomes significant, especially when the designed controller has low bandwidth. Under certain regularity and assumptions regarding the switching signal, the observer's asymptotic stability is shown. Similarly, theoretical observer parameters are determined by considering a simple second-order system's settling time and overshoot properties. Although they are not precisely the same due to switching dynamics of the observer, controller and reference filter characteristics, performed simulations show comparable settling time and overshoot trends. In this sense, controller bandwidth may also affect the friction estimation performance of the observer. Lastly, simulations results demonstrate that although the observer mainly aims to Coulomb coefficient, it improves the system performance evidentially; even existing friction cannot be confined to Coulomb Model only.

We note that we also performed some experiments on the application of the friction observers and the adaptive friction cancellation scheme presented in this work for the position control of some DC motors. More specifically, we utilised both the observer proposed in this paper, as well as the observer mentioned in Remark 2.6, to generate the estimated friction torque given by (3), and then by modifying the DC motor current we attempted to cancel the friction. The required computations are performed by MATLAB Simulink communicating with Arduino Uno based motor controller platform. Although we observed certain improvements in the position tracking error compared to the case where friction is ignored, the results are still premature and need further investigation. The details can be found in Odabaş (2021) for interested readers. Since our main scope in this paper is the structure of the proposed observer and its stability properties, these points are left as a future research problem.

Certainly, friction identification and compensation is a vast research area. As previously mentioned, many friction models and identification techniques have different complexities and effectiveness. In this sense, there are many estimation/identification challenges, such as multiple parameters estimation for accurate identification, parameter identification of dynamic characteristics, and identification of time-varying

parameters in the existing friction. Although the proposed observer design fundamentally focuses on Coulomb coefficient estimation, it also considers the velocity error dynamics without any initial parameter information. As a result, the proposed scheme has a simple adaptive observer structure with two different gains for both friction and velocity estimations. Therefore, without exhaustive identification and design processes, the novel observer can exhibit a promising performance under friction characteristics that are not limited to a simple Coulomb coefficient.

Disclosure statement

No potential conflict of interest was reported by the authors.

ORCID

Caner Odabaş  <http://orcid.org/0000-0002-6890-1003>

Ömer Morgül  <http://orcid.org/0000-0002-3158-3961>

References

- Angeli, D., De Leenheer, P., & Sontag, E. D. (2009). Chemical networks with inflows and outflows: A positive linear differential inclusions approach. *Biotechnology Progress*, 25(3), 632–642. <https://doi.org/10.1002/btpr.162>
- Armstrong-Hélouvy, B., Dupont, P., & de Wit, C. C. (1994). A survey of models, analysis tools and compensation methods for the control of machines with friction. *Automatica*, 30(7), 1083–1138. [https://doi.org/10.1016/0005-1098\(94\)90209-7](https://doi.org/10.1016/0005-1098(94)90209-7)
- Åström, K. J., & Wittenmark, B. (2013). *Adaptive control*. Courier Corporation.
- Baykara, B. (2009). *Control of systems under the effect of friction* [Master's thesis]. Middle East Technical University.
- Bliman, P. A., & Sorine, M. (1993). *A system-theoretic approach to systems with hysteresis. Application to friction modelling and compensation*. Groningen, The Netherlands: Proceedings of the European Control Conference.
- Canudas de Wit, C., Olsson, H., Åström, K. J., & Lischinsky, P. (1995). A new model for control of systems with friction. *IEEE Transactions on Automatic Control*, 40(3), 419–425. <https://doi.org/10.1109/9.376053>
- Cheng, D., Guo, L., Lin, Y., & Wang, Y. (2004). A note on overshoot estimation in pole placements. *Journal of Control Theory and Applications*, 2(2), 161–164. <https://doi.org/10.1007/s11768-004-0062-2>
- Cheng, D., Guo, L., Lin, Y., & Wang, Y. (2005). Stabilization of switched linear systems. *IEEE Transactions on Automatic Control*, 50(5), 661–666. <https://doi.org/10.1109/TAC.2005.846594>
- Dahl, P. R. (1968). *A solid friction model* (Tech. Rep.). Aerospace Corp El Segundo Ca.
- Dorf, R. C., & Bishop, R. H. (2008). *Modern control systems*. Pearson Prentice Hall.
- Friedland, B., & Park, Y. (1992). On adaptive friction compensation. *IEEE Transactions on Automatic Control*, 37(10), 1609–1612. <https://doi.org/10.1109/9.256395>
- Golnaraghi, F., & Kuo, B. C. (2017). *Automatic control systems*. McGraw-Hill Education.
- Graham, D., & Lathrop, R. C. (1953). The synthesis of 'optimum' transient response: criteria and standard forms. *Transactions of the American Institute of Electrical Engineers, Part II: Applications and Industry*, 72(5), 273–288. <https://doi.org/10.1109/TAI.1953.6371346>
- Hensen, R. H. A. (2002). *Controlled mechanical systems with friction* [Doctoral dissertation]. Technische Universiteit Eindhoven.
- Hespanha, J., & Morse, A. (1999). Stability of switched systems with average dwell-time. In *Proceedings of the 38th IEEE conference on decision and control (Cat. No. 99CH36304)* (Vol. 3, pp. 2655–2660). <https://doi.org/10.1109/CDC.1999.831330>
- Hespanha, J. P. (2004). Uniform stability of switched linear systems: Extensions of LaSalle's invariance principle. *IEEE Transactions on Automatic Control*, 49(4), 470–482. <https://doi.org/10.1109/TAC.2004.825641>

- Khalil, H. K. (2002). *Nonlinear systems*. 3rd ed. Prentice-Hall
- Koru, A. T., Delibaşı, A., & Özbay, H. (2018). Dwell time-based stabilisation of switched delay systems using free-weighting matrices. *International Journal of Control*, 91(1), 1–11. <https://doi.org/10.1080/00207179.2016.1266515>
- Lee, H. S., & Tomizuka, M. (1996). Robust motion controller design for high-accuracy positioning systems. *IEEE Transactions on Industrial Electronics*, 43(1), 48–55. <https://doi.org/10.1109/41.481413>
- Le Tien, L., Albu-Schaffer, A., De Luca, A., & Hirzinger, G. (2008). Friction observer and compensation for control of robots with joint torque measurement. In *2008 IEEE/RSJ international conference on intelligent robots and systems* (pp. 3789–3795). <https://doi.org/10.1109/IROS.2008.4651049>
- Morse, A. (1996). Supervisory control of families of linear set-point controllers—Part I. Exact matching. *IEEE Transactions on Automatic Control*, 41(10), 1413–1431. <https://doi.org/10.1109/9.539424>
- Odabaş, C. (2014). *Observer based friction cancellation in mechanical systems* [Master's thesis]. Bilkent University.
- Odabaş, C. (2021). *Adaptive observer designs for friction estimation in position control of simple mechanical systems with time delay* [Doctoral dissertation]. Bilkent University.
- Odabaş, C., & Morgül, Ö. (2014). Observer based friction cancellation in mechanical systems. In *2014 14th international conference on control, automation and systems (ICCAS 2014)* (pp. 12–16). <https://doi.org/10.1109/ICCAS.2014.6987950>
- Odabaş, C., & Morgül, Ö. (2020). Adaptive friction compensations for mechanical systems with measurement delay. *Transactions of the Institute of Measurement and Control*, 43(8), 1745–1759. <https://doi.org/10.1177/0142331220947568>
- Olsson, H., & Astrom, K. J. (1996). Observer-based friction compensation. In *Proceedings of 35th IEEE conference on decision and control* (Vol. 4, pp. 4345–4350). <https://doi.org/10.1109/CDC.1996.577475>
- Olsson, H., Åström, K. J., De Wit, C. C., Gäfvert, M., & Lischinsky, P. (1998). Friction models and friction compensation. *European Journal of Control*, 4(3), 176–195. [https://doi.org/10.1016/S0947-3580\(98\)70113-X](https://doi.org/10.1016/S0947-3580(98)70113-X)
- Pait, F. M., & Morse, A. S. (1994). A cyclic switching strategy for parameter-adaptive control. *IEEE Transactions on Automatic Control*, 39(6), 1172–1183. <https://doi.org/10.1109/9.293177>
- Palli, G., & Melchiorri, C. (2008). Velocity and disturbance observer for non-model based load and friction compensation. In *2008 10th IEEE international workshop on advanced motion control* (pp. 194–199). <https://doi.org/10.1109/AMC.2008.4516065>
- Ray, L. R., Ramasubramanian, A., & Townsend, J. (2001). Adaptive friction compensation using extended Kalman–Bucy filter friction estimation. *Control Engineering Practice*, 9(2), 169–179. [https://doi.org/10.1016/S0967-0661\(00\)00104-0](https://doi.org/10.1016/S0967-0661(00)00104-0)
- Sun, Z., & Ge, S. S. (2011). Stability theory of switched dynamical systems.
- Tafazoli, S., de Silva, C. W., & Lawrence, P. D. (1998). Tracking control of an electrohydraulic manipulator in the presence of friction. *IEEE Transactions Control Systems Technology*, 6(3), 401–411. <https://doi.org/10.1109/87.668040>
- Tan, D., Wang, Y., & Zhang, L. (2007). Research on the parameter identification of LuGre tire model based on genetic algorithms. In *International conference on intelligent systems and knowledge engineering 2007* (pp. 498–502).
- Taşdelen, U., & Özbay, H. (2013). On Smith predictor-based controller design for systems with integral action and time delay. In *2013 9th Asian control conference (ASCC)* (pp. 1–6). <https://doi.org/10.1109/ASCC.2013.6606172>
- Vidyasagar, M. (1978). *Nonlinear systems analysis*. Prentice-Hall.
- Wang, X., & Wang, S. (2011). High performance adaptive control of mechanical servo system with LuGre friction model: Identification and compensation. *Journal of Dynamic Systems, Measurement, and Control*, 134(1). <https://doi.org/10.1115/1.4004785>
- Xie, W. F. (2007). Sliding-mode-observer-based adaptive control for servo actuator with friction. *IEEE Transactions on Industrial Electronics*, 54(3), 1517–1527. <https://doi.org/10.1109/TIE.2007.894718>